ORIGINAL ARTICLE

JBMR

# Hyperlipidemia Induces Resistance to PTH Bone Anabolism in Mice via Oxidized Lipids

Andrew P Sage,[1*] Jinxiu Lu,[2] Elisa Atti,[3] Sotirios Tetradis,[3] Maria-Grazia Ascenzi,[4] Douglas J Adams,[5] Linda L Demer,[1,2,6] and Yin Tintut[1]

[1]Division of Cardiology, Department of Medicine, University of California, Los Angeles, Los Angeles, CA, USA
[2]Department of Physiology, University of California, Los Angeles, Los Angeles, CA, USA
[3]Department of Dentistry, University of California, Los Angeles, Los Angeles, CA, USA
[4]Department of Orthopedic Surgery, University of California, Los Angeles, Los Angeles, CA, USA
[5]Department of Orthopedic Surgery, New England Musculoskeletal Institute, University of Connecticut Health Center, Farmington, CT, USA
[6]Department of Biomedical Engineering, University of California, Los Angeles, Los Angeles, CA, USA

**ABSTRACT**

In hyperlipidemia, oxidized lipids accumulate in vascular tissues and trigger atherosclerosis. Such lipids also deposit in bone tissues, where they may promote osteoporosis. We found previously that oxidized lipids attenuate osteogenesis and that parathyroid hormone (PTH) bone anabolism is blunted in hyperlipidemic mice, suggesting that osteoporotic patients with hyperlipidemia may develop resistance to PTH therapy. To determine if oxidized lipids account for this PTH resistance, we blocked lipid oxidation products in hyperlipidemic mice with an ApoA-I mimetic peptide, D-4F, and the bone anabolic response to PTH treatment was assessed. Skeletally immature $Ldlr^{-/-}$ mice were placed on a high-fat diet and treated with D-4F peptide and/or with intermittent PTH(1–34) injections. As expected, D-4F attenuated serum lipid oxidation products and tissue lipid deposition induced by the diet. Importantly, D-4F treatment attenuated the adverse effects of dietary hyperlipidemia on PTH anabolism by restoring micro–computed tomographic parameters of bone quality—cortical mineral content, area, and thickness. D-4F significantly reduced serum markers of bone resorption but not bone formation. PTH and D-4F, together but not separately, also promoted bone anabolism in an alternative model of hyperlipidemia, $Apoe^{-/-}$ mice. In normolipemic mice, D-4F cotreatment did not further enhance the anabolic effects of PTH, indicating that the mechanism is through its effects on lipids. These findings suggest that oxidized lipids mediate hyperlipidemia-induced PTH resistance in bone through modulation of bone resorption. © 2011 American Society for Bone and Mineral Research.

**KEY WORDS:** OXIDIZED LIPIDS; HYPERLIPIDEMIA; PARATHYROID HORMONE; OSTEOANABOLISM; OSTEOPOROSIS

## Introduction

Hyperlipidemia, resulting from mutations in low-density lipoprotein receptor or apolipoprotein E, has adverse effects on the vasculature, including development of atherosclerosis and vascular calcification. Under hyperlipidemic conditions, low-density lipoprotein (LDL) particles cross the endothelial barrier and are trapped in the subendothelial space, where they undergo nonenzymatic oxidative modification owing to production of reactive oxygen species by metabolically active neighboring smooth muscle cells and macrophages.[1] Since bone and its marrow are both vascularized, a similar process appears to occur in human osteoporotic bone, with oxidized lipoprotein particles accumulating in the perivascular subendothelial spaces.[2] Osteoblasts also have the capacity to oxidatively modify lipoproteins,[3] and products of lipid oxidation are detected in the marrow of hyperlipidemic mice.[2,3] A high-fat diet further increases lipoprotein levels and their oxidative products.[4,5] Importantly, regardless of whether from a genetic or a dietary source, lipid oxidation products attenuate osteogenic differentiation in vitro.[6–8] In mice, hyperlipidemia induces bone loss[9,10] and impairs the anabolic effects[11] of intermittent parathyroid hormone (PTH), a regimen now used for the treatment of osteoporosis.

These effects of hyperlipidemia may account for the clinical association of osteoporosis with hyperlipidemia. According to data from the National Health and Nutrition Examination Survey (NHANES III), 63% of osteoporotic patients have

Received in original form May 21, 2010; revised form October 13, 2010; accepted December 1, 2010. Published online December 15, 2010.
Address correspondence to: Yin Tintut, PhD, Division of Cardiology, David Geffen School of Medicine, University of California Los Angeles, Center for the Health Sciences, A2-237, 10833 Le Conte Avenue, Los Angeles, CA 90095-1679, USA. E-mail: ytintut@mednet.ucla.edu
*Present Address for APS: University of Cambridge, Division of Cardiovascular Medicine, Addenbrookes Hospital, Cambridge, CB2 0QQ, United Kingdom

Journal of Bone and Mineral Research, Vol. 26, No. 6, June 2011, pp 1197–1206
DOI: 10.1002/jbmr.312

hyperlipidemia.[12] Serum lipid levels negatively correlate with whole-body bone mineral content (BMC)[13] and bone mineral density (BMD) and mass.[14,15] Though not confirmed in prospective, randomized trials, observational studies suggest that lipid-lowering agents reduce fracture risk.[16,17] In animal models, diet-induced hyperlipidemia is associated with a reduction in BMD and BMC in both mice and canines.[9,18,19]

High-density lipoprotein (HDL) functions as an anti-inflammatory and antiatherosclerotic agent through reverse cholesterol transport of oxidized lipids from lipid-laden cells. The effects of HDL are mediated through its apoprotein components, including ApoA-I.[20] Navab and colleagues have demonstrated that ApoA-I itself removes lipid hydroperoxides from LDL and that, in mice, injection of ApoA-I results in LDL that is resistant to oxidation.[5] Recently, a number of ApoA-I-mimetic peptides, such as D-4F, an 18-amino-acid class-A amphipathic helical peptide, have been found to display enhanced lipid-binding capabilities compared with ApoA-I.[21] Treatment of *Apoe*$^{-/-}$ mice with D-4F promotes HDL function and inhibits lipid oxidation without affecting total lipid levels, resulting in reduced atherosclerotic lesions.[22,23] In this study, we tested the hypothesis that reducing serum lipid oxidation by treatment with the ApoA-I-mimetic peptide D-4F would rescue PTH anabolism in mice with genetic and diet-induced hyperlipidemia.

## Methods

*Ldlr*$^{-/-}$ and *Apoe*$^{-/-}$ mice (both on a C57BL/6 background) and wild-type (C57BL/6) mice were obtained from the Jackson Laboratory (Bar Harbor, ME, USA). The experimental protocol was reviewed and approved by the Institutional Animal Care and Use Committee of the University of California at Los Angeles.

### *Ldlr*$^{-/-}$ mouse study

As shown in Fig. 1, 28 female mice were started on an atherogenic high-fat diet (HFD; 20.5% kcal from protein, 42.4% kcal from carbohydrate, 37.1% kcal from fat, formulated in pellets; TD 90221; Harlan Teklad, Madison, WI, USA) at 10 weeks of age. At 16 weeks of age, half the mice were given D-4F (100 μg/mL) via drinking water until termination of the experiment. D-4F was synthesized as described previously.[24] At 20 weeks of age, half of each group was given daily (5 days/week) subcutaneous injections of PBS or PTH [hPTH(1–34), 40 μg/kg; Sigma, St Louis, MO, USA] for 3 weeks. To compare effects of the HFD versus chow diet, a separate control group of *Ldlr*$^{-/-}$ mice (8 females) was maintained on a chow diet and not treated with either PTH or D-4F. At the end of the experiment, animals were euthanized, and sera and tissues were collected.

Femurs and tibias were carefully harvested and cleaned of soft tissues. For computed tomography, tibias were stored in 70% ethanol at 4°C, and for histomorphometry, femurs were fixed in 70% ethanol, dehydrated, and embedded undecalcified in methyl methacrylate. Tibias (6/group, chosen at random; *Ldlr*$^{-/-}$) were analyzed for length, BMC, BMD, cortical area, and cortical thickness by micro–computed tomography (μCT; Skyscan 1172, Aartselaar, Belgium). The data were collected at 55 kVp and 72 μA at a resolution of 12 μm. Volumetric analysis was performed using the Skyscan software. For cortical analysis at the mid-diaphysis, the length of each tibial bone was determined, and 40 mid-diaphyseal slices were used. For trabecular bone analysis, 200 slices per tibia were measured, covering a total of 2.4 mm from the proximal

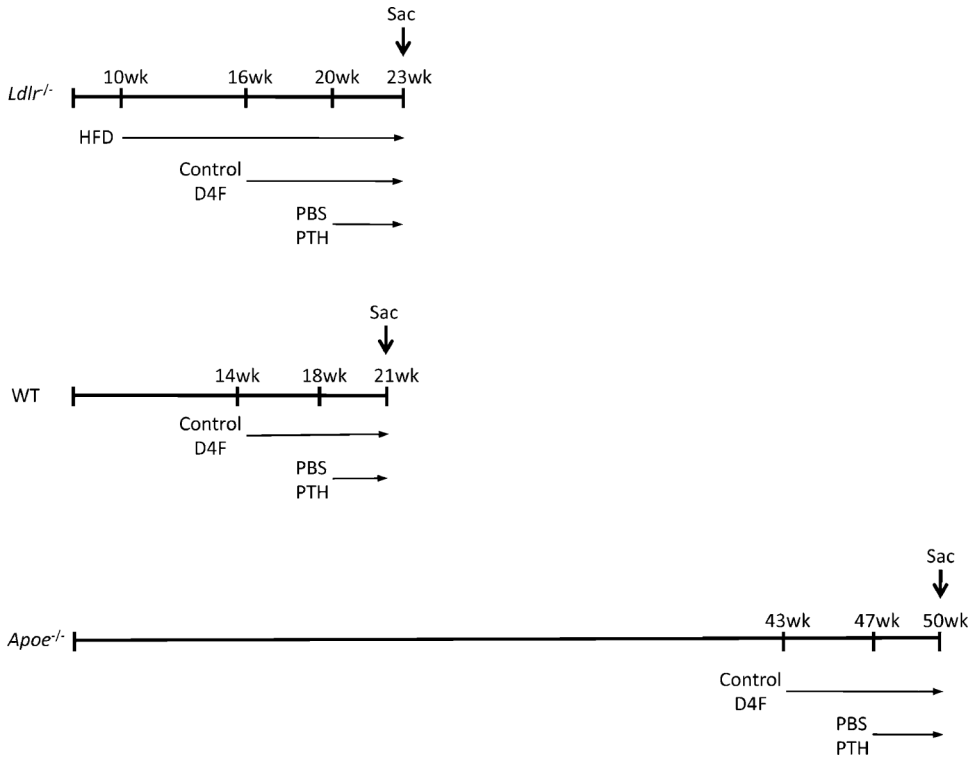


**Fig. 1.** Diet and treatment protocols. Schematic diagram of diet and treatment regimen (in weeks from birth) for *Ldlr*$^{-/-}$, wild-type, and *Apoe*$^{-/-}$ mice.

growth plate to the shaft distally. The analysis of the secondary spongiosa begins at 0.048 mm below the most distal point of the primary spongiosa, which was defined as directly distal to the most distal portion of the growth plate. A hydroxyapatite phantom was used for BMD calibration.

To assess growth plate thickness, paraffin-embedded sections (5 μm) of tibias were stained with hematoxylin and eosin and examined using digital photomicrography and image-processing software (MetaMorph for Olympus, Version 7.7, Olympus America Inc., Center Valley, PA, USA). We acquired images of the central 1-mm horizontal dimension of the growth plate at ×10 magnification and automated edge detection to determine the edges of the growth plate and measured the average vertical thickness in pixels. Values were normalized as a percent of those for chow-fed animals.

Thick longitudinal cryosections (60 μm, 6 sections/diet group) of the tibial bones were observed under circularly polarized light (×30 to ×100) with a Leitz Dialux 20 microscope (Midland, ON, Canada) equipped with two crossed Nicol's prisms, one above and one below the specimen, and a λ/4 compensator to eliminate the Maltese cross effect. Circularly polarized lights detect the anisotropy of bone through "bright" and "extinct" signals owing to birefringence (double refraction) of collagen.[25] For quantitation of the birefringence signal, illumination intensity and the threshold for distinguishing bright and extinct signal were constant for all specimens; then percent area occupied by bright birefringence signals at the proximal, middle, and distal tibia was quantitated with MetaMorph software (Molecular Devices, Sunnyvale, CA, USA).

Spleen, kidney, and decalcified femoral bone tissues were embedded in 22-oxacalcitrol (OCT compound). Cryosections (10 μm, 4 sections/mouse, 2 to 3 mice/group) were used for oil red O staining and counterstained with hematoxylin using standard histologic methods.

### Histomorphometric analysis of trabecular bone

Six femurs, randomly chosen from chow and HFD groups, were subjected to static histomorphometry. Longitudinal sections (5 μm thick) were cut with a microtome (Microm, Richards-Allan Scientific, Kalamazoo, MI, USA) and stained with toluidine blue (pH 6.4). Parameters of bone formation and resorption were measured in a defined area between 181 and 725 μm below the growth plate using the OsteoMeasure Morphometry System (Osteometrics, Atlanta, GA, USA). The terminology and units used are those recommended by the Histomorphometry Nomenclature Committee of the American Society for Bone and Mineral Research. Data from two femurs of the HFD group were excluded owing to compromised cell visualization, which likely resulted from insufficient fixation.

### Serum biochemical assays

Serum lipid oxidation products were assayed by dichlorofluorescein (DCF) assay, as described previously.[26] The indicator, 2′,7′-dichlorodihydrofluorescein diacetate ($H_2$DCFDA; Invitrogen, Carlsbad, CA, USA), is sensitive to reactive oxygen species such as lipid oxidation products; oxidation removes its acetate groups, producing an intense fluorescent signal.[26] Briefly, serum samples (from 7 chow, 4 PBS, 4 PTH/D-4F, 5 PTH, and 3 D-4F mice) were incubated with $H_2$DCFDA at 37°C. The fluorescence (excitation 485 nm, emission 530 nm), a quantitative measure of lipid oxidation products, was monitored over 1 hour. Oxidized 1-palmitoyl-2-arachidonoyl-sn-glycero-3-phosphocholine (ox-PAPC) was used to generate a standard curve. Serum levels of osteocalcin (Biomedical Technologies, Inc., Stoughton, MA, USA), insulin-like growth factor 1 (IGF-1; IDS Inc., Fountain Hills, AZ, USA), procollagen type 1 N-terminal propeptide (P1NP; Immunodiagnostic Systems), tartrate-resistant acid phosphatase 5b (TRACP-5b; Immunodiagnostic Systems) were measured in quadruplicate.

### C57BL/6 mouse study

C57BL/6 mice (14 week-old females) were given a standard Purina chow diet. The animals were treated with either normal water ($n = 7$) or D-4F-containing water ($n = 7$) for 7 weeks and were injected with vehicle or hPTH(1–34) (5 days/week) for 3 weeks (Fig. 1). μCT morphometry was performed on the tibial mid-diaphysis ($n = 7$/group), as mentioned earlier. The slight difference in age from the *Ldlr*$^{-/-}$ mice was unintentional.

### *Apoe*$^{-/-}$ mouse study

*Apoe*$^{-/-}$ mice (43-week-old females) on a C57BL/6 background were given a standard Purina chow diet. The animals were treated with either normal water ($n = 8$) or D-4F-containing water ($n = 8$) for 7 weeks and were injected with vehicle or hPTH(1–34) (5 days/week) for 3 weeks (Fig. 1). μCT morphometry was performed on the femoral mid-diaphysis ($n = 6$/group) at the University of Connecticut. Briefly, *Apoe*$^{-/-}$ femurs (6/group, chosen at random) were imaged using cone-beam, microfocus X-ray computed tomography (μCT40, Scanco Medical AG, Bassersdorf, Switzerland). Serial tomographic images were acquired at 55 kV and 145 μA, collecting 1000 projections per rotation at 300-ms integration time. Then 3D 16-bit grayscale images were reconstructed using standard convolution, back-projection algorithms with Shepp and Logan filtering and rendered within a 12.3-mm field of view at a discrete density of 578,704 voxels/mm$^3$ (isometric 12-μm voxels). Segmentation of cortical bone from marrow and soft tissue was performed in conjunction with a constrained Gaussian filter to reduce noise, applying a hydroxyapatite-equivalent density threshold of 700 mg/cm$^3$.

### Real-time RT-qPCR

Total RNA was isolated from the calvaria of chow and HFD groups (4/group). Real-time reverse-transcriptase polymerase chain reaction (RT-qPCR) was performed using the One-Step qRT-PCR SuperMix Kit (BioChain Institute, Inc., Hayward, CA, USA) and Mx3005P Real-Time PCR System (Agilent Technologies, Inc., Wilmington, DE, USA), as described previously.[27–29]

### Statistical analysis

HFD effects on gene expression and bone parameters were compared in chow versus HFD groups by Student's *t* test. Comparisons across more than two groups were performed with two-way ANOVA, followed by the Fisher's PLSD test using

StatView (Version 4.5, Abacus, Berkeley, CA, USA). Values are expressed as means ± SEM. A value of $p \leq .05$ is considered statistically significant.

## Results

### Effect of the HFD on gene expression

Since lipid oxidation products inhibit bone-forming cells in vitro,[6,8,10] we first tested the effects of an HFD on bone cell differentiation markers in *Ldlr*$^{-/-}$ mice on a C57BL/6 background. This HFD was previously shown by Towler and colleagues to increase atherogenic lipoproteins in this mouse model.[30] Real-time RT-qPCR of the calvarial tissues showed that the HFD significantly reduced expression of bone-formation markers, PTH receptor, core binding factor α1 (Cbfa-1), bone sialoprotein, and osteocalcin (Fig. 2*A*). Treatment with PTH or D-4F or cotreatment did not restore their expression (data not shown). In addition, HFD significantly reduced expression of the osteoclast inhibitor osteoprotegerin (OPG; Fig. 2*A*); however, treatment with PTH or D-4F or cotreatment did not restore OPG expression (data not shown). HFD did not significantly affect receptor activator of NF-kB ligand (RANKL) expression (Fig. 2*A*); however, both PTH and PTH/D-4F cotreatment significantly induced RANKL expression compared with HFD alone (data not shown).

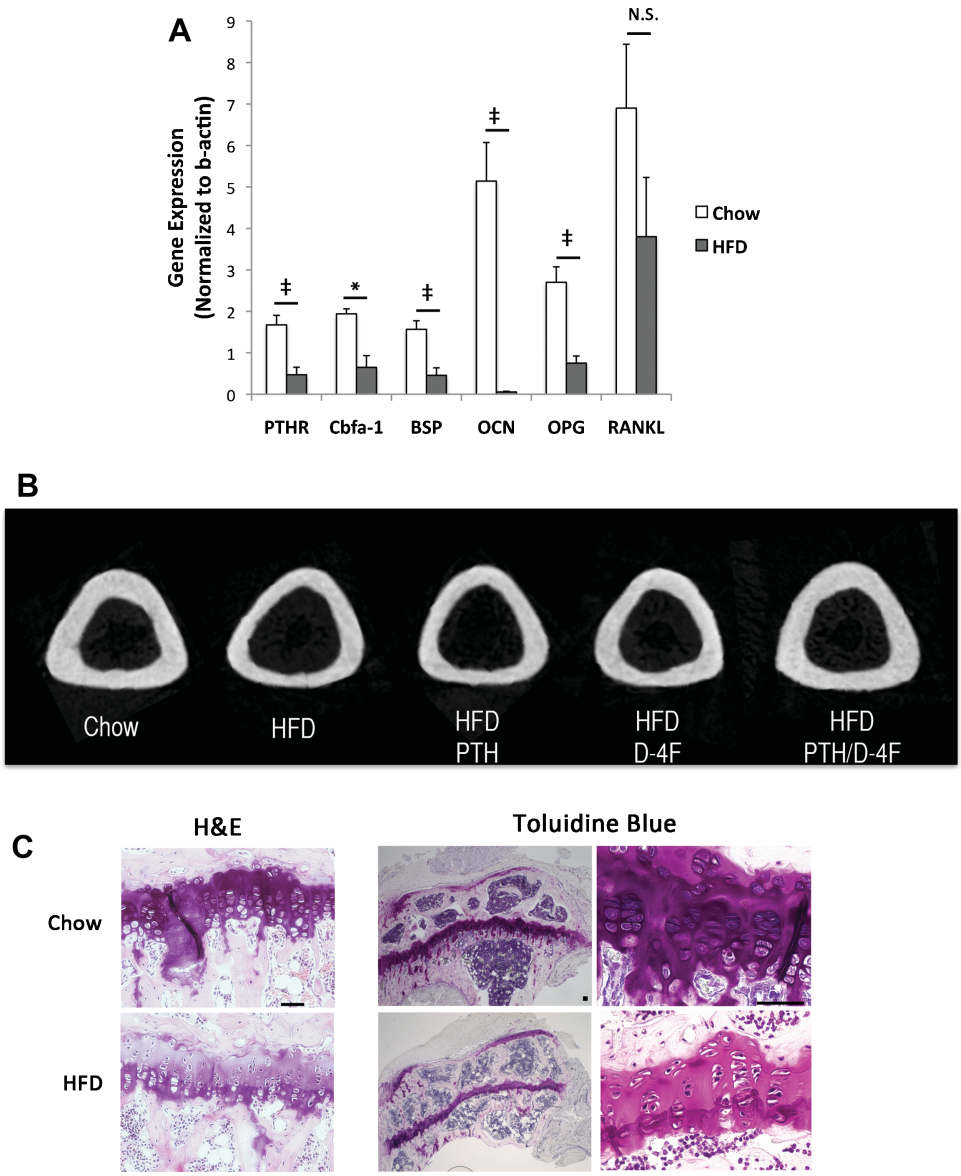


**Fig. 2.** Effect of HFD in *Ldlr*$^{-/-}$ mice. (*A*) Real-time RT-qPCR analysis of RNA from calvarial tissues of chow or high-fat diet (HFD) groups for *PTH receptor 1* (*PTHR*), *core binding factor α1* (*Cbfa-1*), *bone sialoprotein* (*BSP*), *osteocalcin* (*OCN*), *osteoprotegerin* (*OPG*) *and receptor-activator of NF-kB ligand* (*RANKL*). (*B*) 2D reconstruction of μCT analysis of tibial midshaft. (*C*) Hematoxylin and eosin (H&E) and toluidine blue staining of tibial metaphyses from chow and HFD mice (scale bar = 50 μm). (*D*) Circularly polarized light microscopy of coronal section of proximal tibia (scale bar = 100 μm). Extinct (*arrowhead*) and bright signals (*arrow*) indicate predominant collagen orientation < 45 degrees and > 45 degrees, respectively, to the long axis of the bone. Arrowheads and arrows indicate equivalent locations in each image. Quantitation of bright birefringence signals (% area) in the proximal tibia. $^{*}p < .05$; $^{\ddagger}p < .01$; $^{**}p < .005$; $^{\#}p < .001$; NS = not significant.

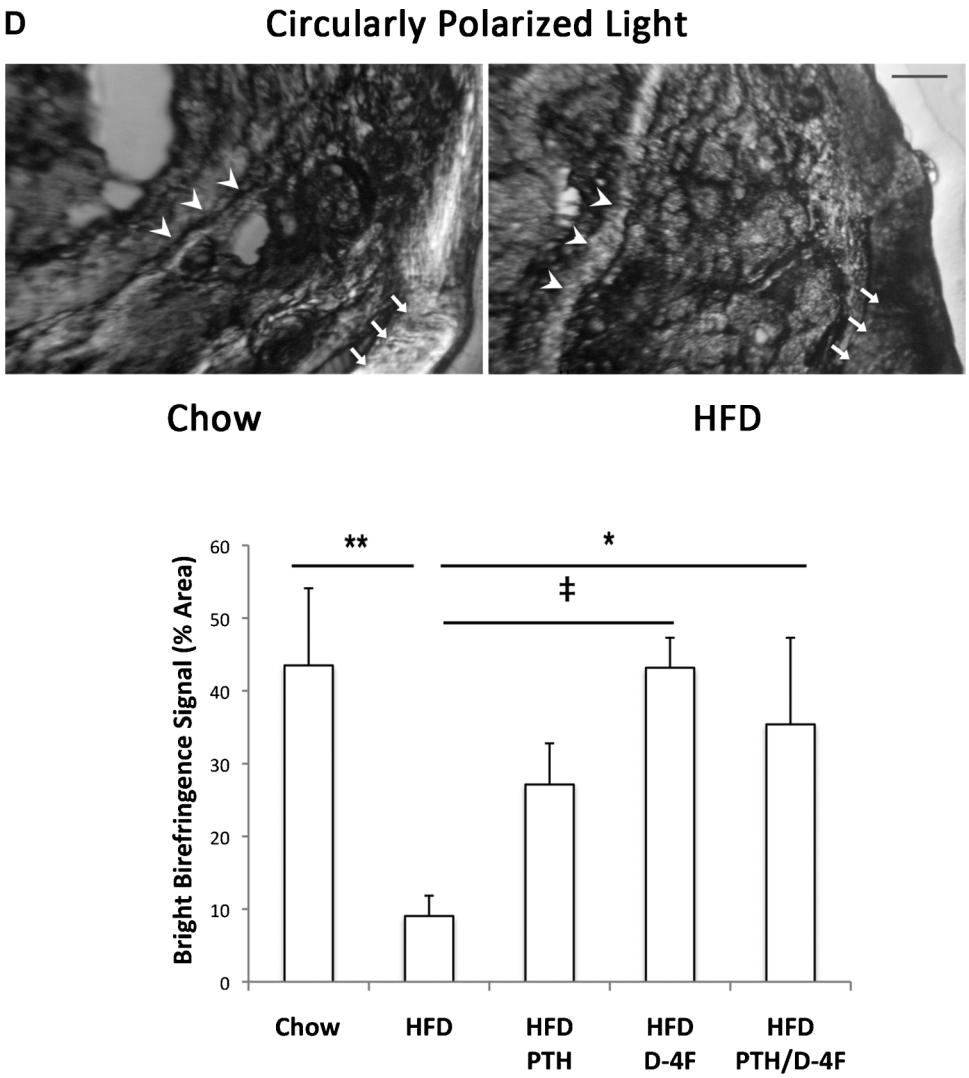


**Fig. 2.** (*Continued*)

## Effect of the HFD on bone

μCT analysis showed that the HFD reduced tibial length (Table 1) and cortical bone thickness (Fig. 2*B*) in these skeletally immature mice. Histologic analysis showed that HFD also had a nonsignificant trend toward reduced thickness ($p = .1$; Table 1) and size of hypertrophic chondrocytes in the tibial growth plate (Fig. 2*C*). Collagen anisotropy was assessed by extinct versus bright signals of circularly polarized light, which are generated, respectively, by collagen fibrils that align nearly parallel to the loading axis versus those with other orientations.[31] In HFD mice and controls, we found that the extinct/bright patterns were reversed at the corresponding regions of tension and compression (Fig. 2*D*). At the proximal but not at the middle or distal tibial cortex, the bright birefringence signals were reduced significantly by the HFD, which was restored by D-4F treatment (Fig. 2D).

**Table 1.** Tibial Bone Length and Growth Plate Thickness of *Ldlr*$^{-/-}$ Mice

| Treatment | Length (mm) | Growth plate thickness (% of control) |
|---|---|---|
| Chow | $18.5 \pm 0.09$ | $100 \pm 12$ |
| HFD | $17.8 \pm 0.08^*$ | $44 \pm 21$ |
| HFD + PTH | $17.9 \pm 0.13^*$ | $44 \pm 24$ |
| HFD + D-4F | $17.8 \pm 0.09^*$ | $46 \pm 26$ |
| HFD + PTH + D-4F | $17.8 \pm 0.11^*$ | $66 \pm 19$ |

$^*p < 0.0005$ versus chow.

## Effect of the HFD and D-4F on lipid oxidation and accumulation

We found previously that bone anabolic effects of PTH are impaired in hyperlipidemic mice.[11] To test whether the PTH resistance in hyperlipidemic mice could be normalized by reducing serum lipid oxidation products, mice on the HFD were treated with D-4F (or vehicle) for 4 weeks, followed by 3 weeks of daily PTH(1–34) or PBS injections with continuation of D-4F or vehicle treatments and the HFD (Fig. 1). Serum lipid oxidation products were assayed using DCF, as described previously.[26] As shown in Fig. 3*A*, the HFD significantly increased fluorescence intensity, which was reduced significantly by D-4F treatment (D-4F and PTH/D-4F), consistent with previous findings.[24] Oil red O

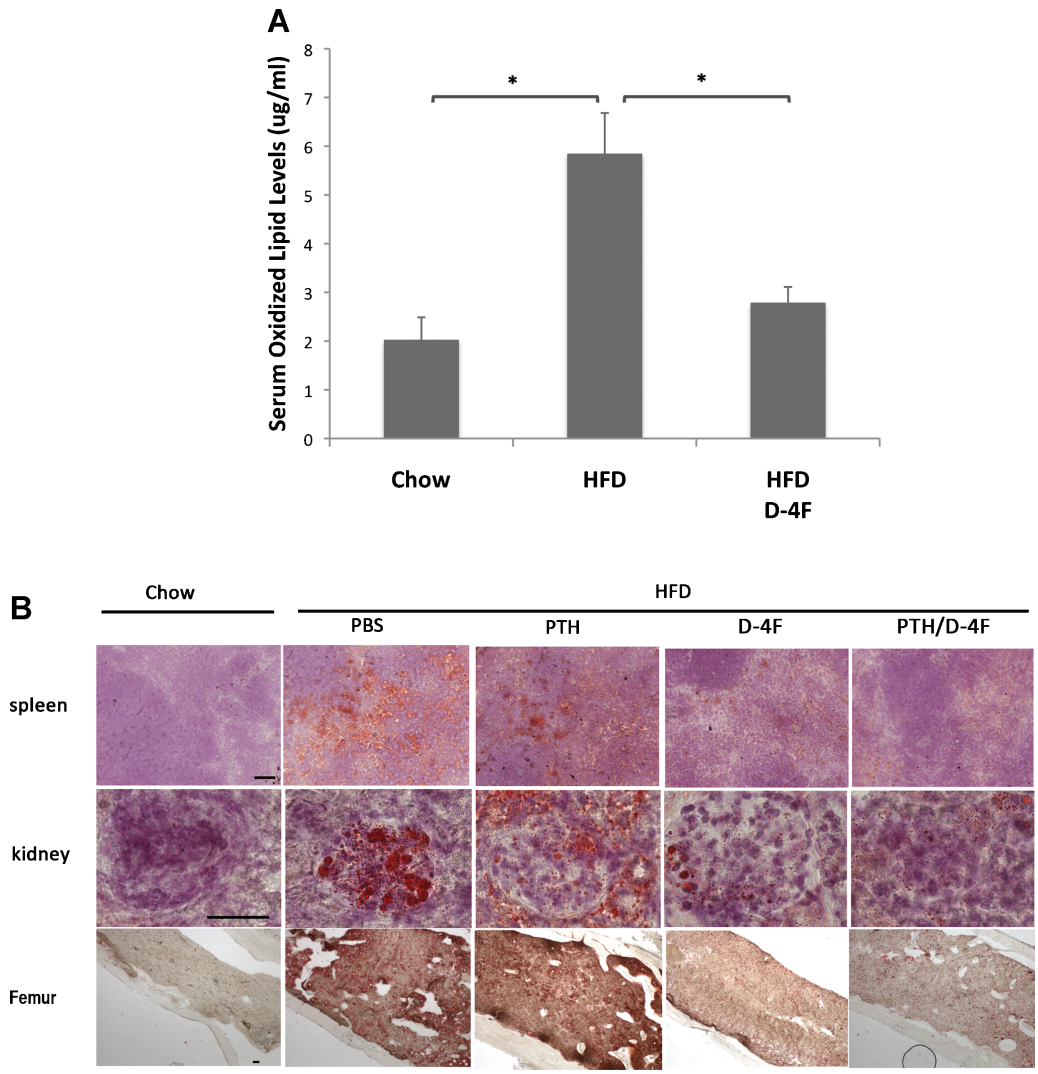


**Fig. 3.** Effect of D-4F on lipid oxidation and deposition in *Ldlr*$^{-/-}$ mice. (*A*) Dichlorofluorescein (DCF) assay for lipid oxidation products in chow, HFD (PBS and PTH), and D-4F (PTH/D-4F and D-4F) groups. (*B*) Oil red O staining for lipids (*red*) in spleen, kidney, and femoral bone cryosections counterstained with hematoxylin. Scale bar = 50 μm. $^{*}p < .05$.

staining in spleen, kidney, and femoral bone tissues indicated that the HFD also caused substantial lipid accumulation, which was reduced significantly by D-4F treatment alone or with PTH cotreatment (Fig. 3*B*).

## Effect of the ApoA-I-mimetic peptide on HFD-induced PTH resistance

μCT analysis of cortical bone parameters at the mid-diaphyseal tibia of *Ldlr*$^{-/-}$ mice showed that the HFD significantly reduced cortical area, thickness, and BMC (Figs. 2*B* and 4*A*). These adverse effects were retarded by PTH/D-4F cotreatment but not by PTH or D-4F treatment alone. This is in contrast to normolipemic wild-type mice, where treatment with PTH alone, but not D-4F alone, augmented cortical area, thickness, and BMC, and cotreatment with D-4F did not further enhance PTH anabolic effects (Table 2). Histomorphometric analysis of trabecular bone parameters at the metaphyseal femur showed that both PTH and PTH/D-4F treatments induced trabecular bone volume and numbers of trabeculae (Fig. 4*B*). The trabecular thickness lost with the HFD also was restored by both PTH and PTH/D-4F treatments (Fig. 4*B*). Histomorphometric analysis of osteoclast numbers and osteoclast surface areas were not significantly different among the groups (data not shown). Bone-formation parameters, such as osteoid, osteoblast number, and osteoblast surface area, were not included in the analysis owing to zero values in some HFD mice not receiving PTH. We therefore analyzed serum markers for bone formation (ie, osteocalcin and P1NP) and resorption (ie, TRACP-5b), respectively. As shown in Fig. 4*C*, the HFD did not alter serum levels of these three markers. Intermittent PTH treatment resulted in a twofold increase in serum levels of the two bone-formation markers and a slight (1.4%) increase in the bone-resorption marker compared with PBS controls. PTH/D-4F cotreatment resulted in the same twofold increase in bone-formation markers relative to PBS control but a decrease in TRACP-5b (45% versus PBS control and 59% versus PTH; Fig. 4*C*). D-4F treatment alone also decreased TRACP-5b by 44% without altering the serum levels of osteocalcin and P1NP (Fig. 4*C*). We next determined the effect of the HFD on serum IGF-1 levels and its mRNA expression in calvarial tissues. Interestingly, HFD

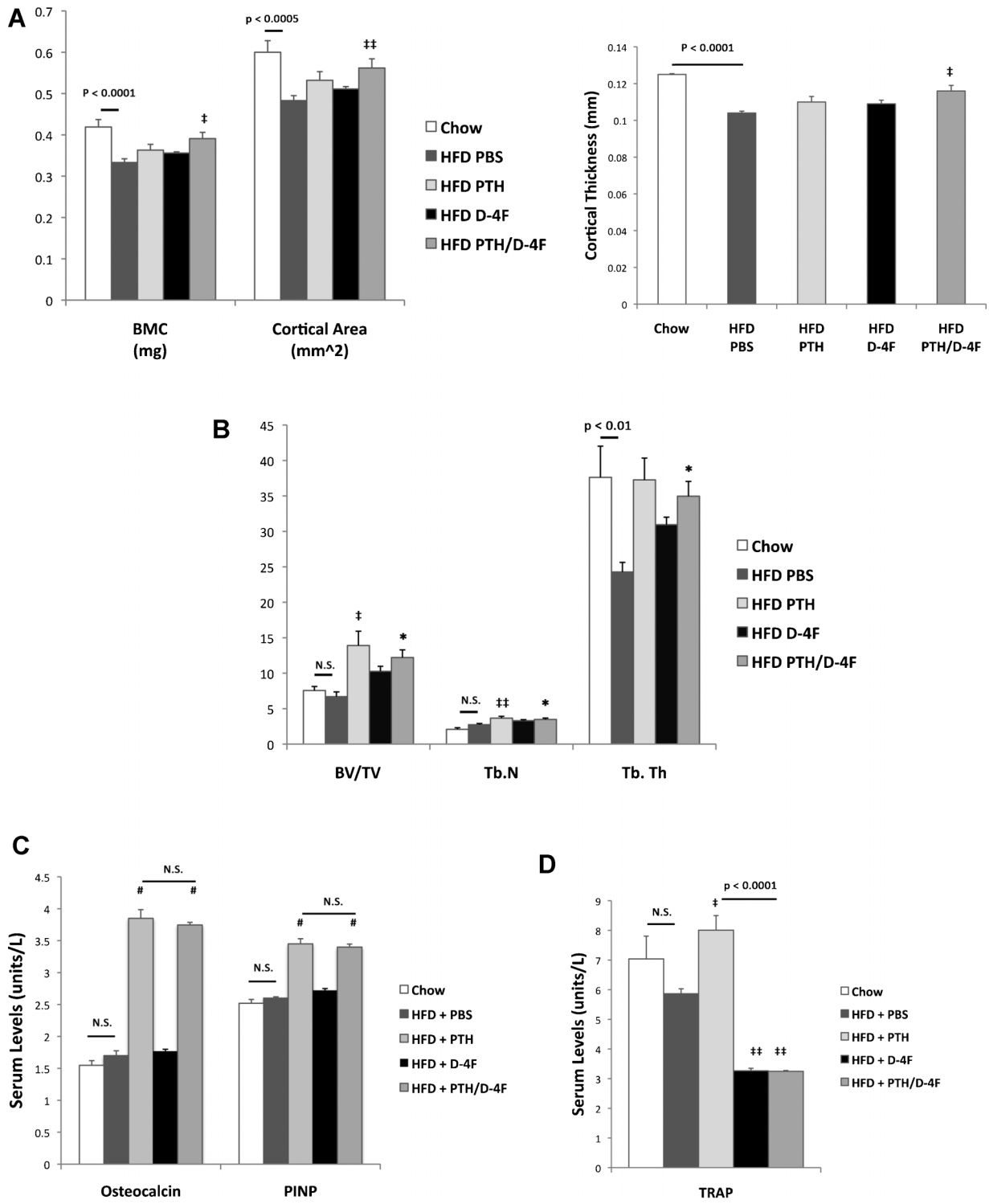


**Fig. 4.** Effect of D-4F in *Ldlr*$^{-/-}$ mice. (*A*) μCT analysis of tibial cortical BMC, area, and thickness. (*B*) Histomorphometric analysis of trabecular bone volume/tissue volume (BV/TV), number (Tb.N), and thickness (Tb.Th). (*C*) Serum levels of bone-formation markers osteocalcin and procollagen type 1 N-terminal propeptide (P1NP). (*D*) Serum levels of the bone-resorption marker TRACP-5b. $^{*}p < .05$; $^{‡‡}p < .01$; $^{‡}p < .005$; $^{‡‡}p < .001$; $^{\#}p < .0001$ versus HFD/PBS; N.S. = not significant.

induced serum IGF-1 levels but reduced IGF-1 expression in calvarial tissue (Table 3). Serum IGF-1 levels also were induced by the D-4F alone treatment but not by PTH alone or by the cotreatment with D-4F (Table 3).

The experiments also were conducted in a second hyperlipidemic mouse model, *Apoe*$^{-/-}$, on the same C57BL/6 background. Eleven-month-old *Apoe*$^{-/-}$ mice were treated with D-4F for 4 weeks, followed by either vehicle or hPTH(1–34) daily (5 days/week) for 3 weeks with continued D-4F treatment (Fig. 1), and femoral bones were scanned by μCT. Consistent with the results in HFD-treated *Ldlr*$^{-/-}$ mice, cotreatment with PTH/D-4F significantly increased the same cortical bone parameters (ie,

**Table 2.** μCT Analysis of Tibial Bone in Wild-Type (C57BL/6) Mice

| Treatment (mm) | Bone mineral content (mg) | Cortical area ($mm^2$) | Cortical thickness |
|---|---|---|---|
| PBS | $0.46 \pm 0.01$ | $0.657 \pm 0.012$ | $0.132 \pm 0.002$ |
| PTH | $0.49 \pm 0.00^{\ddagger}$ | $0.713 \pm 0.007^{*}$ | $0.137 \pm 0.001^{\ddagger}$ |
| D4F | $0.47 \pm 0.01$ | $0.666 \pm 0.010$ | $0.130 \pm 0.002$ |
| PTH/D4F | $0.48 \pm 0.01$ | $0.696 \pm 0.017^{\ddagger}$ | $0.135 \pm 0.002$ |

$^{\ddagger}p < .05$; $^{*}p < .005$ versus PBS.

**Table 3.** IGF-1 Levels in *Ldlr*$^{-/-}$ Mice

| Treatment | Serum IGF-1 (ng/mL) | Calvarial *Igf1* mRNA (normalized to β-actin) |
|---|---|---|
| Chow | $323 \pm 13$ | $2.79 \pm 0.10$ |
| HFD | $397 \pm 15^{*}$ | $1.46 \pm 0.20^{\ddagger}$ |
| HFD + PTH | $434 \pm 29^{**}$ | $1.42 \pm 0.21^{**}$ |
| HFD + D-4F | $469 \pm 38^{**,\#}$ | $1.32 \pm 0.12^{**}$ |
| HFD + PTH + D-4F | $376 \pm 32^{\ddagger\ddagger}$ | $1.42 \pm 0.17^{\ddagger}$ |

$^{\ddagger\ddagger}p < .05$; $^{*}p < .005$; $^{**}p < .0001$; $^{\ddagger}p < .0005$ versus chow; $^{\#}p < .005$ versus HFD.

BMC, cortical area, and cortical thickness), whereas neither D-4F nor PTH alone affected these parameters (Table 4).

## Discussion

It is well known in cardiovascular biology that a diet high in fat promotes atherogenesis[32] by increasing levels of lipid oxidation products,[4,5] especially in genetically hyperlipidemic subjects. It is now recognized that such a diet also reduces bone density,[9,18,19] promotes bone resorptive activity,[2,9,33,34] and importantly, interferes with parenteral PTH therapy.[11] Using two hyperlipidemic mouse models, we now report the first evidence that lipid oxidation products mediate hyperlipidemia-induced PTH resistance and that this resistance is overcome by a known inhibitor of the bioactivity of lipid oxidation products, the ApoA-I-mimetic peptide D-4F. In normolipemic wild-type mice, D-4F did not augment PTH anabolic effects, further supporting the concept that D-4F acts through its effects on lipids.

Our studies suggest that the HFD has adverse effects on bone growth. Our findings of shortened bone length and matrix maturation in the skeletally immature mice on the HFD are consistent with previous reports that show that bone length and maturation are reduced in the offspring of pregnant mice fed a diet high in fat.[35] In addition, our findings are consistent with recent reports that show small size as well as decreased height in preadolescents and adolescents with hyperlipidemia,[36,37] supporting the need for further investigation into the regulatory mechanism of this phenomenon. Interestingly, changes in serum IGF-1 levels did not correspond with the changes in bone formation. This could be explained in part by recent findings of Elis and colleagues[38] that show that serum IGF-1 levels synergize PTH action only when the tissue IGF-1 is intact/sufficient. Indeed, we found that tissue IGF-1 expression was reduced significantly in HFD mice.

Our studies also suggest that the HFD alters bone quality. Collagen anisotropy has been shown to contribute to mechanical integrity and bone "quality" and to differ between regions in tension and in compression in normal and osteomalacic human bone exposed to normal activity.[25] Our findings suggest that the HFD disrupts collagen orientation. Such loss of microstructural, coordinated alignment is known to associate with loss of bone strength, bending stiffness, and fracture toughness in mice fed an HFD.[39]

Our results and those of Hirasawa and colleagues[9] indicate that the combination of genetic hyperlipidemia and HFD causes more rapid bone loss than either condition alone.[18] Using an ApoA-I-mimetic peptide to inhibit lipid oxidation,[22,24] we now provide evidence that the mechanism by which an HFD leads to PTH resistance is through generation of lipid oxidation products. We have found previously that oxidized lipids induce osteoclastogenesis directly[33] and also indirectly via osteoblastic production of inflammatory cytokines, including interleukin 6 (IL-6). Our findings show that this peptide normalized PTH anabolism in two hyperlipidemic mouse strains owing, in part, to inhibition of osteoclastic activity. Although D4-F alone might be expected to inhibit bone loss in HFD mice, no inhibition was observed, presumably because D-4F was started later than the HFD. However, D-4F treatment did show a trend in preventing bone loss, suggesting that suppression of oxidized lipids is involved in the HFD-induced bone loss. Our findings also suggest that D-4F is not an anabolic factor and that its effects appear to be primarily through effects on bone resorption.

**Table 4.** μCT Analysis of Femoral Bone in *Apoe*$^{-/-}$ Mice

| | Bone mineral content (μg) | Cortical area ($mm^2$) | Cortical thickness (mm) |
|---|---|---|---|
| PBS | $11.5 \pm 0.6$ | $0.667 \pm 0.042$ | $0.152 \pm 0.007$ |
| PTH | $11.9 \pm 0.06$ | $0.717 \pm 0.031$ | $0.157 \pm 0.008$ |
| D4F | $11.4 \pm 0.07$ | $0.683 \pm 0.031$ | $0.150 \pm 0.009$ |
| PTH/D4F | $13.2 \pm 0.03^{*}$ | $0.767 \pm 0.021^{*}$ | $0.178 \pm 0.005^{*}$ |

$^{*}p < .05$ versus PBS.

Interestingly, the adverse effect of hyperlipidemia-induced PTH resistance is less prominent in trabecular bone. Consistent with our previous studies,[11] we found that the adverse effects of hyperlipidemia on PTH anabolism are greater in cortical than trabecular bone, suggesting that metabolic activity to maintain serum calcium is less affected. The exact mechanism governing this difference is unclear. However, one possibility may lie in the differences in COX-2 signaling in cortical versus trabecular bone. Xu and colleagues recently showed that cortical, but not trabecular, bone parameters are reduced in *Cox2* knockout mice.[40] It is also interesting to note that oxidized lipids induce COX-2 expression in monocytes,[41] and prostaglandins produced by COX-2 stimulate bone resorption.[33,42] Further studies are required to address this mechanism.

In summary, these results suggest that the large proportion of osteoporotic patients who have hyperlipidemia may not be receiving the full benefits of anabolic therapy. Clinical studies may be warranted to investigate the efficacy of PTH therapy in patients with disorders of lipid metabolism.

## Disclosures

M-GA is the chief scientist of Micro-Generated Algorithms, LLC. All the other authors state that they have no conflicts of interest.

## Acknowledgments

This research was supported by grants from the National Institutes of Health (DK076009, DK081346, DK081346-S1, and HL081202) and the Laubisch Endowment at UCLA. We thank M Huang, L Hon, G Hough, F Ye, and JW Combs for their expert technical assistance, Dr R Pereira (UCLA Bone Histomorphometric Laboratory) for histomorphometric analysis, and Dr M Navab for guidance.

## References

1. Navab M, Berliner JA, Watson AD, et al. The yin and yang of oxidation in the development of the fatty streak: a review based on the 1994 George Lyman Duff Memorial Lecture. Arterioscler Thromb Vasc Biol. 1996;16:831–842.
2. Tintut Y, Morony S, Demer LL. Hyperlipidemia promotes osteoclastic potential of bone marrow cells ex vivo. Arterioscler Thromb Vasc Biol. 2004;24:e6–10.
3. Brodeur MR, Brissette L, Falstrault L, Ouellet P, Moreau R. Influence of oxidized low-density lipoproteins (LDL) on the viability of osteoblastic cells. Free Radic Biol Med. 2008;44:506–517.
4. Laurila A, Cole SP, Merat S, et al. High-fat, high-cholesterol diet increases the incidence of gastritis in LDL receptor-negative mice. Arterioscler Thromb Vasc Biol. 2001;21:991–996.
5. Navab M, Hama SY, Cooke CJ, et al. Normal high density lipoprotein inhibits three steps in the formation of mildly oxidized low density lipoprotein: step 1. J Lipid Res. 2000;41:1481–1494.
6. Almeida M, Ambrogini E, Han L, Manolagas SC, Jilka RL. Increased lipid oxidation causes oxidative stress, increased peroxisome proliferator-activated receptor-gamma expression, and diminished pro-osteogenic Wnt signaling in the skeleton. J Biol Chem. 2009;284:27438–27448.
7. Mody N, Parhami F, Sarafian TA, Demer LL. Oxidative stress modulates osteoblastic differentiation of vascular and bone cells. Free Radic Biol Med. 2001;31:509–519.
8. Parhami F, Morrow AD, Balucan J, et al. Lipid oxidation products have opposite effects on calcifying vascular cell and bone cell differentiation. A possible explanation for the paradox of arterial calcification in osteoporotic patients. Arterioscler Thromb Vasc Biol. 1997;17:680–687.
9. Hirasawa H, Tanaka S, Sakai A, et al. ApoE gene deficiency enhances the reduction of bone formation induced by a high-fat diet through the stimulation of p53-mediated apoptosis in osteoblastic cells. J Bone Miner Res. 2007;22:1020–1030.
10. Parhami F, Jackson SM, Tintut Y, et al. Atherogenic diet and minimally oxidized low density lipoprotein inhibit osteogenic and promote adipogenic differentiation of marrow stromal cells. J Bone Miner Res. 1999;14:2067–2078.
11. Huang MS, Lu J, Ivanov Y, et al. Hyperlipidemia impairs osteoanabolic effects of PTH. J Bone Miner Res. 2008;23:1672–1679.
12. Bilezikian JP, Davidson M, Hendrix S, Liu L, Louie M. Co-Morbidity of Decreased Bone Mineral Density (BMD) and Increased Cholesterol Levels among Women Aged 65 Years and Older: Results from NHANES III. ASBMR 27th Annual Meeting. 2005; SU130.
13. Li X, Yang HY, Giachelli CM. Role of the sodium-dependent phosphate cotransporter, Pit-1, in vascular smooth muscle cell calcification. Circ Res. 2006;98:905–912.
14. Tanko LB, Bagger YZ, Christiansen C. Low bone mineral density in the hip as a marker of advanced atherosclerosis in elderly women. Calcif Tissue Int. 2003;73:15–20.
15. Wu S, De Luca F. Role of cholesterol in the regulation of growth plate chondrogenesis and longitudinal bone growth. J Biol Chem. 2004;279:4642–4647.
16. Edwards CJ, Hart DJ, Spector TD. Oral statins and increased bone-mineral density in postmenopausal women. Lancet. 2000;355:2218–2219.
17. Meier CR, Schlienger RG, Kraenzlin ME, Schlegel B, Jick H. HMG-CoA reductase inhibitors and the risk of fractures. JAMA. 2000;283:3205–3210.
18. Parhami F, Tintut Y, Beamer WG, Gharavi N, Goodman W, Demer LL. Atherogenic high-fat diet reduces bone mineralization in mice. J Bone Miner Res. 2001;16:182–188.
19. Turek JJ, Watkins BA, Schoenlein IA, Allen KG, Hayek MG, Aldrich CG. Oxidized lipid depresses canine growth, immune function, and bone formation. J Nutr Biochem. 2003;14:24–31.
20. Shah PK, Yano J, Reyes O, et al. High-dose recombinant apolipoprotein A-I(milano) mobilizes tissue cholesterol and rapidly reduces plaque lipid and macrophage content in apolipoprotein e-deficient mice. Potential implications for acute plaque stabilization. Circulation. 2001;103:3047–3050.
21. Van Lenten BJ, Wagner AC, Jung CL, et al. Anti-inflammatory apoA-I-mimetic peptides bind oxidized lipids with much higher affinity than human apoA-I. J Lipid Res. 2008;49:2302–2311.
22. Buga GM, Frank JS, Mottino GA, et al. D-4F decreases brain arteriole inflammation and improves cognitive performance in LDL receptor-null mice on a Western diet. J Lipid Res. 2006;47:2148–2160.
23. Navab M, Anantharamaiah GM, Hama S, et al. D-4F and statins synergize to render HDL antiinflammatory in mice and monkeys and cause lesion regression in old apolipoprotein E-null mice. Arterioscler Thromb Vasc Biol. 2005;25:1426–1432.
24. Navab M, Anantharamaiah GM, Reddy ST, et al. Oral D-4F causes formation of pre-beta high-density lipoprotein and improves high-density lipoprotein-mediated cholesterol efflux and reverse cholesterol transport from macrophages in apolipoprotein E-null mice. Circulation. 2004;109:3215–3220.

25. Ascenzi MG, Lomovtsev A. Collagen orientation patterns in human secondary osteons, quantified in the radial direction by confocal microscopy. J Struct Biol. 2006;153:14–30.
26. Navab M, Hama SY, Hough GP, Subbanagounder G, Reddy ST, Fogelman AM. A cell-free assay for detecting HDL that is dysfunctional in preventing the formation of or inactivating oxidized phospholipids. J Lipid Res. 2001;42:1308–1317.
27. Huang MS, Morony S, Lu J, et al. Atherogenic phospholipids attenuate osteogenic signaling by BMP-2 and parathyroid hormone in osteoblasts. J Biol Chem. 2007;282:21237–21243.
28. Huang MS, Sage AP, Lu J, Demer LL, Tintut Y. Phosphate and pyrophosphate mediate PKA-induced vascular cell calcification. Biochem Biophys Res Commun. 2008;374:553–558.
29. Morony S, Tintut Y, Zhang Z, et al. Osteoprotegerin inhibits vascular calcification without affecting atherosclerosis in ldlr(−/−) mice. Circulation. 2008;117:411–420.
30. Towler DA, Bidder M, Latifi T, Coleman T, Semenkovich CF. Diet-induced diabetes activates an osteogenic gene regulatory program in the aortas of low density lipoprotein receptor-deficient mice. J Biol Chem. 1998;273:30427–30434.
31. Ascenzi MG, Gill J, Lomovtsev A. Orientation of collagen at the osteocyte lacunae in human secondary osteons. J Biomech. 2008; 41:3426–3435.
32. Furnkranz A, Schober A, Bochkov VN, et al. Oxidized phospholipids trigger atherogenic inflammation in murine arteries. Arterioscler Thromb Vasc Biol. 2005;25:633–638.
33. Tintut Y, Parhami F, Tsingotjidou A, Tetradis S, Territo M, Demer LL. 8-Isoprostaglandin E2 enhances receptor-activated NFkappa B ligand (RANKL)-dependent osteoclastic potential of marrow hematopoietic precursors via the cAMP pathway. J Biol Chem. 2002;277:14221–14226.
34. Xiao Y, Cui J, Li YX, et al. Dyslipidemic high-fat diet affects adversely bone metabolism in mice associated with impaired antioxidant capacity. Nutrition. 2010; DOI: 10.1016/j.nut.2009.11.012.
35. Liang C, Oest ME, Jones JC, Prater MR. Gestational high saturated fat diet alters C57BL/6 mouse perinatal skeletal formation. Birth Defects Res B Dev Reprod Toxicol. 2009;86:362–369.
36. Knudsen VK, Orozova-Bekkevold IM, Mikkelsen TB, Wolff S, Olsen SF. Major dietary patterns in pregnancy and fetal growth. Eur J Clin Nutr. 2008;62:463–470.
37. Patel A, Pyzik PL, Turner Z, Rubenstein JE, Kossoff EH. Long-term outcomes of children treated with the ketogenic diet in the past. Epilepsia. 2010;51:1277–1282.
38. Elis S, Courtland HW, Wu Y, et al. Elevated serum IGF-1 levels synergize PTH action on the skeleton only when the tissue IGF-1 axis is intact. J Bone Miner Res. 2010;25:2051–2058.
39. Ionova-Martin SS, Do SH, Barth HD, et al. Reduced size-independent mechanical properties of cortical bone in high-fat diet-induced obesity. Bone. 2010;46:217–225.
40. Xu M, Choudhary S, Voznesensky O, et al. Basal bone phenotype and increased anabolic responses to intermittent parathyroid hormone in healthy male COX-2 knockout mice. Bone. 2010;47:341–352.
41. Pontsler AV, St Hilaire A, Marathe GK, Zimmerman GA, McIntyre TM. Cyclooxygenase-2 is induced in monocytes by peroxisome proliferator activated receptor gamma and oxidized alkyl phospholipids from oxidized low density lipoprotein. J Biol Chem. 2002;277:13029–13036.
42. Tsukii K, Shima N, Mochizuki S, et al. Osteoclast differentiation factor mediates an essential signal for bone resorption induced by 1 alpha,25-dihydroxyvitamin D3, prostaglandin E2, or parathyroid hormone in the microenvironment of bone. Biochem Biophys Res Commun. 1998;246:337–341.